Synthesis and Characterization of Nano-Tungsten Oxide Precipitated onto Natural Inorganic Clay for Humidity-Sensing Applications

ceramics

MDPI

Article

Synthesis and Characterization of Nano-Tungsten Oxide Precipitated onto Natural Inorganic Clay for Humidity-Sensing Applications

Ahmed S. Afify [1,*], Ahmed Elsayed [1,2], Mohamed Hassan [3], Mohamed Ataalla [4], Amr Mohamed [5,6], Azhar Hussain [1,7], Ahmad S. Abu-Khadra [8] and Jean-Marc Tulliani [1]

1 Department of Applied Science and Technology, Politecnico di Torino, Corso Duca degli Abruzzi, 24, 10129 Torino, Italy; ahmed.elsayed@polito.it (A.E.); azharhussain@uettaxila.edu.pk (A.H.); jeanmarc.tulliani@polito.it (J.-M.T.)
2 Department of Conservation, Faculty of Archaeology, Sohag University, Sohag 82524, Egypt
3 High Institute for Engineering & Technology, 21 K Cairo-Belbeis Rd, Al-Obour 11828, Egypt; dr.m.qader@oi.edu.eg
4 Faculty of Engineering and Technology, Badr University in Cairo (BUC), Badr 11829, Egypt; mohamed.sobhi@buc.edu.eg
5 Department of Chemistry, Faculty of Science, Taibah University, Al-Madinah 41411, Saudi Arabia; amr_deck@hotmail.com
6 The Higher Institute of Optics Technology (HIOT), Heliopolis, Cairo 17361, Egypt
7 Department of Metallurgy and Materials Engineering, UET, Taxila, Punjab 47050, Pakistan
8 Department of Basic Science, Faculty of Engineering Science, Sinai University, North Sinai 45615, Egypt; ahmad.sabrry@su.edu.eg
* Correspondence: ahmed.afify@polito.it; Tel.: +966547249717

Received: 28 May 2018; Accepted: 10 July 2018; Published: 12 July 2018

Abstract: A wet chemical method was used to obtain tungsten oxide nanoparticles from tungsten tetrachloride and natural microfibrous inorganic clay (sepiolite) as a starting material. Precipitation of tungsten oxide species onto sepiolite under basic conditions and subsequent thermal treatment was investigated, prompted by the abundance of sepiolite in nature and the useful environmental applications that could be attained. Laser granulometry, X-ray diffraction, field emission scanning electron microscopy (FE-SEM), energy dispersive X-ray spectroscopy (EDX), and high-resolution transmission electron microscopy (HR-TEM) techniques were used to study the particle-size distribution, the morphology, and the composition of the prepared sample. Our findings show the presence of tungsten oxide nanoparticles, which are less than 50 nm, on the needles of the modified sepiolite.

Keywords: HRTEM; nanoparticles; precipitation; sepiolite; tungsten oxide

1. Introduction

Over the last decades, nanotechnologies have received great attention because they allow the synthesis of one-dimensional structures, including nanorods, nanobelts, and nanowires, which play crucial roles in the relationship between size, morphology, and featured characteristics of the powder. Transition metals and metal oxides are interesting functional materials for growing nanoparticles with a specific shape. They are widely used in many applications, such as sensors, catalysts, ceramics, solar cells, electrical devices, etc. [1,2]. Tungsten oxide is a very important semiconductor among transition metal oxides group due to its wide use of applications, such as in gas sensors [3,4], catalysts [5], photochemistry [6], and electrochromic devices [7].

Since the 1990s, a lot of effort has been made to produce tungsten oxide powders at submicron and ultrafine grades, with particle sizes of 0.5 μm [8]. Sepiolite is a microfibrous clay (it is a hydrous magnesium silicate having the chemical formula $Mg_8Si_{12}O_{30}(OH)_4(H_2O)_4{\cdot}8H_2O$). Its structural units are composed of two tetrahedral silica sheets and a discontinuous central layer of octahedral magnesium oxide. This structure provides for the possibility of forming open channels with dimensions of 0.36×1.06 nm^2.

Many methods have been devoted to the preparation of nanoscale tungsten oxide powders, including physical and chemical techniques, such as sol–gel [9,10], physical vapor deposition (PVD) [11], chemical vapor deposition (CVD) [12], spray pyrolysis techniques [13], etc. Most of these techniques have a high cost, are time-consuming, and are processed at high temperatures. Finding an economically viable chemical method which offers the possibility to tailor the size, shape of the structure, and the degree of crystallinity is crucial. Using clays as metal ion supports is economically favorable due to the large deposits of clay minerals in nature and the promising applications that can be targeted, with a potential impact on the society, such as gas and humidity sensors for environmental monitoring [14,15]. In our previous research, we managed to synthesize a nanopowder of zinc oxide which was grown onto the needles of modified sepiolite, and their particle sizes were less than 10 nm [16].

In this study, a simple and low-cost chemical synthesis method with a short preparation time was developed to exploit the abundancy of inorganic clays and metal salts to precipitate nanocrystals of tungsten oxide onto sepiolite grains. The prepared powder was then characterized by means of laser granulometry, X-ray diffraction, field emission scanning electron microscopy (FE-SEM), energy dispersive X-ray spectroscopy (EDX), and high-resolution transmission electron microscopy (HR-TEM) techniques.

2. Materials and Methods

2.1. Preparation of the Materials

All the reagents were ACS grade supplied from Sigma-Aldrich, while natural sepiolite was produced from TOLSA (Pangel S9, Spain). Five grams of sepiolite were first dispersed into distilled water at 10 wt % concentration. Then, the pH of the suspension was set to zero by 37% HCl addition, followed by stirring of the dispersion for 2 h at room temperature to ensure Mg leaching without completely destroying the sepiolite structure [17–19]. In fact, the leached quantity is proportional to the soaking time, temperature, and concentration of the acid, and the sepiolite phase disappears over time [17–19].

The obtained suspension was vacuum filtered, followed by washing with distilled water (2–3 times). After that, the sepiolite powder was mixed with 1.0 L of aqueous solution using 0.75 g of tungsten(IV) tetrachloride, where the pH of the dispersion was adjusted with sodium hydroxide to 10 to ensure that all the tungsten ion species were precipitated [17]. After stirring the dispersion for 20 min, the obtained dispersion was dried overnight at 105 °C. Finally, calcination of the dried powder was performed under static air at 550 °C for 1 h with a heating rate of 2 °C/min.

2.2. Characterization of the Material

A laser granulometer (Malvern 3600D, Worcestershire, Great Britain) was used to determine the particle-size distribution of the pristine sepiolite and of the calcined powder after dispersion in ethanol and sonication for 10 min. X-ray diffraction patterns were collected on calcined powder by means of an X'Pert HighScore Philips analytical diffractometer equipped with a Cu anticathode (λ Cu Kα anticathode = 0.154056 nm). Samples were scanned at a rate of 0.02°/s in the range from 5° to 70° in 2θ. Specific surface area (SSA), total porous volume (Vp), and average pore diameter (Dp) were determined by nitrogen physisorption at −196 °C (Micrometrics ASAP 2020, Micromeritics Instrument Corp., Norcross, GA, USA) on samples previously outgassed at 200 °C for 4 h to remove water and

other atmospheric contaminants. Sample SSAs were calculated using the BET method, and pore diameters were estimated by applying the Barrett–Joyner–Halenda (BJH) algorithm to the isotherm desorption branch.

Finally, the morphology of the powders was observed by means of a FE-SEM (Zeiss Merlin, Oberkochen, Germany), and then by means of an HRTEM (JEOL 3010-UHR instrument; acceleration potential: 300 kV and LaB6 filament) equipped with an Oxford INCA X-ray energy dispersive spectrometer (X-EDS) with a Pentafet Si(Li) detector.

3. Results

3.1. Particle-Size Distribution

Table 1 reports the values corresponding to the 10%, 50%, and 90% cumulative distribution after sonication. It can be seen that the tungsten-modified sepiolite treated at 550 °C for 1 h has a narrower particle-size distribution than pure sepiolite. The reduction of the particles size for the tungsten-modified sepiolite may be due to the strong leaching process, which probably segmented the original sepiolite needles into smaller fragments.

Table 1. Diameter in microns of sepiolite and tungsten-modified sepiolite powders.

Cumulative wt %	Sepiolite (μm)	W-Modified Sepiolite (μm)
10%	6.2	4.8
50%	16.3	11.6
90%	56.7	43.4

3.2. X-ray Diffraction

XRD patterns of pure sepiolite, 2 h leached sepiolite with acid, and tungsten-modified sepiolite after heat treatment at 550 °C for 1 h are reported in Figure 1. The XRD pattern of pure sepiolite was indexed with JCPDS card n°13-595, while the leached heat-treated sample was identified as anhydrous sepiolite [18].

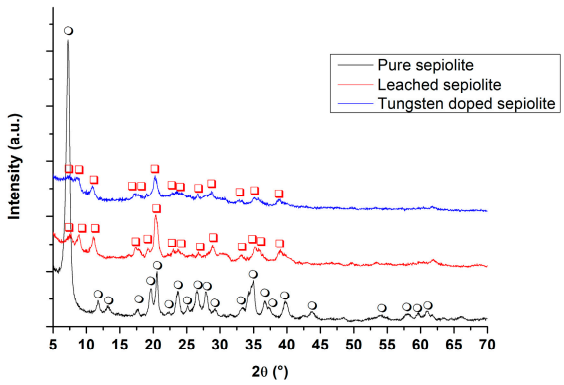

Figure 1. XRD pattern of pristine sepiolite, leached sepiolite, and heat-treated anhydrous sepiolite (○: sepiolite (JCPDS card n°13-595), □: anhydrous sepiolite [18]). Reprinted with permission from [20].

The formation of the anhydrous sepiolite structure is evident in Figure 1 when comparing both X-ray diffraction patterns of pristine sepiolite and of thermally treated powder [17]. In addition, several reflections, such as the reflection of the main peak of the pristine sepiolite that occurs at 1.200 nm (7.36° in 2θ, (110)) and the reflections at 0.757 nm (11.68° in 2θ, (130)), 0.662 nm (13.36° in 2θ, (040)), and 1.970 nm (4.48° in 2θ, (060)) disappeared, whereas two new reflection peaks at 0.999 nm (8.84° in 2θ, (110)) and 0.795 nm (11.12° in 2θ, (120)) corresponding to the folded monoclinic structure

appeared [18]. In this case, the reflection of the main peak occurs at 0.439 nm (20.21° in 2θ, (121)). The presence of both folded and unfolded sepiolite was verified (Figure 1), so results confirm the crystallinity of the modified sepiolite and the formation of nanosized channels in the structure of the anhydrous sepiolite.

3.3. BET Measurements

Specific surface area of the 2 h leached sepiolite was equal to 136 m^2/g, while after tungsten oxide/hydroxide precipitation, an increase of SSA was observed, leading to the final powder having a specific surface area of 155 m^2/g. The increase in SSA is, however, limited (about 14%).

3.4. FE-SEM Observation

The morphologies of the treated powders were observed by FE-SEM, as shown in Figure 2a–c. It is well known that sepiolite is composed of needle-like fibers which are generally assembled in bundles, and these units form dense aggregates. It can be seen in the micrographs that there is no significant difference between the samples—before and after leaching and thermal treatment—in agreement with XRD measurements.

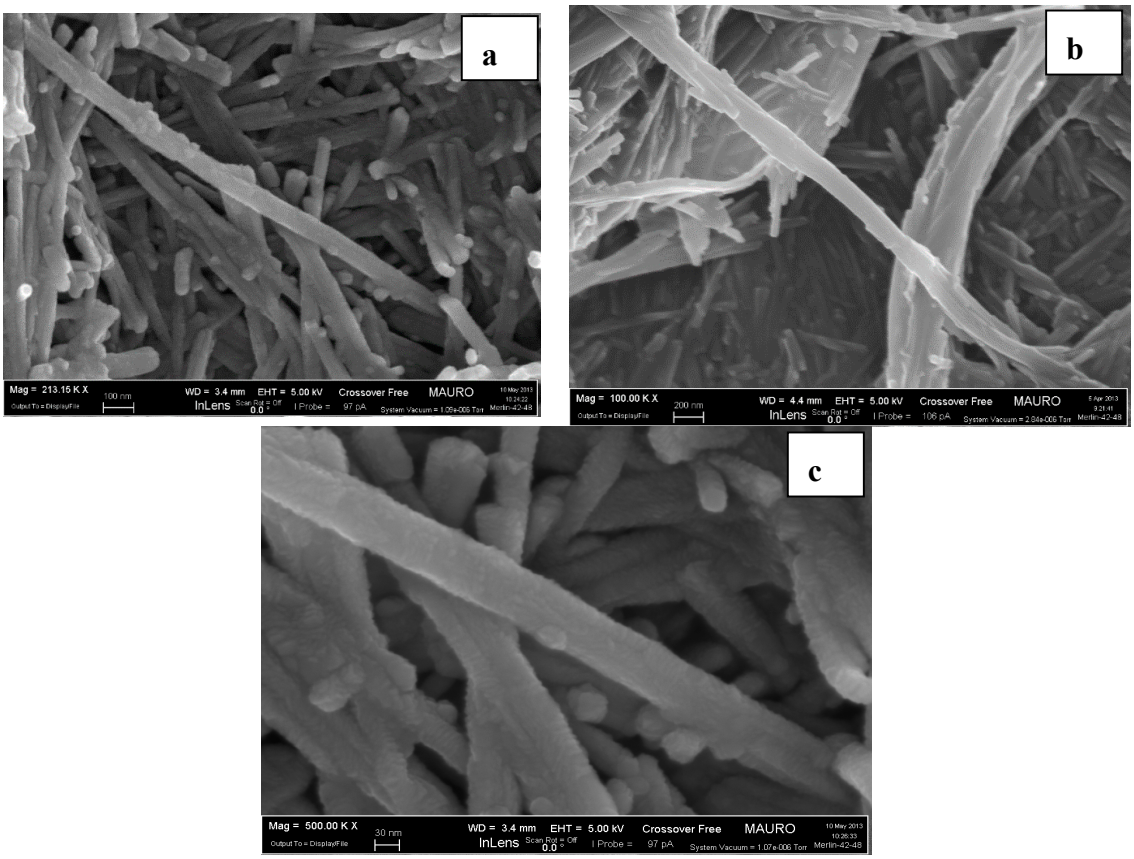

Figure 2. FE-SEM micrographs of: pure sepiolite (**a**); sepiolite thermally treated at 550 °C for 1 h (**b**); tungsten-modified sepiolite after firing at 550 °C for 1 h (**c**).

3.5. Energy Dispersive X-ray Spectroscopy (EDX)

Table 2 shows the semi-quantitative elemental analysis of tungsten-modified sepiolite. Tungsten and magnesium ions were well distributed (map not shown here), and the analysis indicates that tungsten content was about 6.1 atom % in the investigated sample. After acid treatment, the atomic

Mg/Si ratio was about 3 times below the theoretical one of pure sepiolite, indicating a strong magnesium leaching.

Table 2. EDX analysis semi-quantitative results of tungsten-modified sepiolite sample.

Metals	Atom %
Mg	16
Si	77.9
W	6.1

3.6. HRTEM Observation

It can be seen in Figure 3a that modified sepiolite is crystalline, and this result is in good agreement with XRD patterns (Figure 1). Additionally, tungsten nanoparticles can be observed in Figure 3b as nanospheres located on the surface of the needles of modified sepiolite and have a diameter of about 35 nm. The lattice fringes measured on 3 grains of tungsten oxide are around 0.60 ± 0.01 nm.

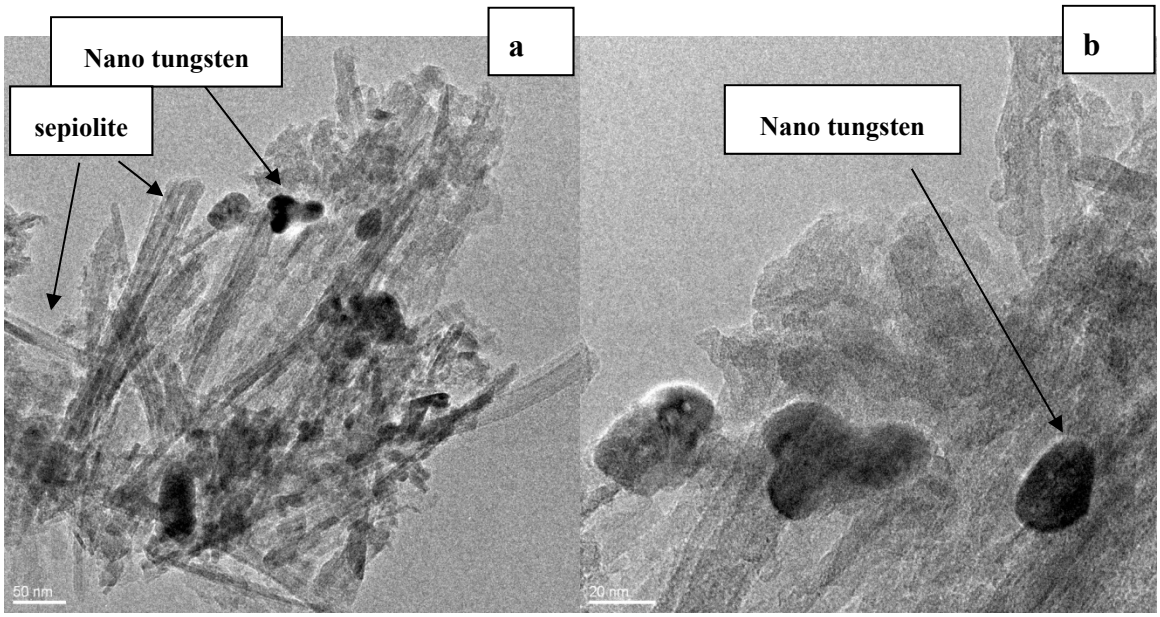

Figure 3. HRTEM of tungsten-modified sepiolite: (**a**) low and (**b**) high magnification.

4. Discussion

Acid treatment of sepiolite removes Mg^{2+} located in its octahedral layer but leaves Si^{4+} coordinated in its tetrahedral layer [17] and turns the Si–O–Mg–O–Si bond into two Si–O–H bonds [18]. Then, the internal channels are connected, and the specific surface area increases. When most magnesium ions are removed, micropores and mesopores expand to macropores, and silica is formed [18]. When it has formed, all the ribbons that comprise the structure are not interconnected, because some of them have lost their octahedral sheet, forming a layer structure [18]. Therefore, a channel structure coming from the sepiolite crystal and a sheet structure corresponding to silica coexist in a single fiber. Thus, only ribbons present on the channel structure fold, whereas unconnected neighboring silica does not participate in this process. Hence, the torque necessary to fold the structure is not exerted, and the crystal remains unfolded with the open channels, but without coordination of water molecules. This organization stabilizes the structure of the original sepiolite [18]. Tungsten phases (tungsten oxide/hydroxide [21]) were not detected in the XRD patterns of Figure 1, either because of their low quantities or because they overlap with the broad peaks of the leached

sepiolite centered at 23.6° and at 28.9° in 2θ. However, the measured lattice fringes in Figure 3 are rather close to the (−301) plane spacing of the monoclinic $W_{18}O_{49}$ compound (0.61 nm), according to JCPDS card n°36-0101 or to the (111) plane of the cubic $WO_3.0.5H_2O$ phase (0.592 nm), according to JCPDS card n°44-0363 or to (111) plane of the cubic $W_{1.5}O_{5.5}H_2{\cdot}H_2O$, according to JCPDS card n°48-0719. Considering these possible candidate phases, it is rather difficult to imagine that crystallized water is still present after the thermal treatment at 550 °C for 1 h. Thus, reasonably, the observed tungsten grains in Figure 3 are probably due to the $W_{18}O_{49}$ compound.

Precipitation of $W_{18}O_{49}$ nanoparticles of tungsten oxide onto the sepiolite matrix by using tungsten tetrachloride as a starting material was successfully done by means of a simple and low-cost wet chemical route. The nanoparticles of tungsten oxide were probably formed from a hydroxide phase precipitated onto sepiolite needles, owing to the soda addition increasing the pH to 10 after magnesium leaching. HRTEM micrographs showed that the particle size of tungsten oxide is about 35 nm in diameter. The authors believe that tungsten ions do not substitute magnesium ions in the leached sepiolite: Mg^{2+} ions are in coordination 4 in the sepiolite structure [21], thus their ionic radius is bigger than ionic radius of W^{6+} ions in the same coordination [22]. Overall, considering the differences in the ionic radii and in the electric charge, the probability that magnesium ions could be replaced by tungsten ions is rather low, if not null. The powder showed a significant sensitivity towards humidity: once screen-printed onto a-Al_2O_3 substrates with platinum electrodes, the sensors showed a response starting from about 40% relative humidity at room temperature, as reported in Figure 4 and documented in a previous work [20]. The difference in the sensing behavior is not only due to the rather limited increase of SSA, but also to tungsten oxide nanoparticle precipitation on the surface of leached sepiolite grains.

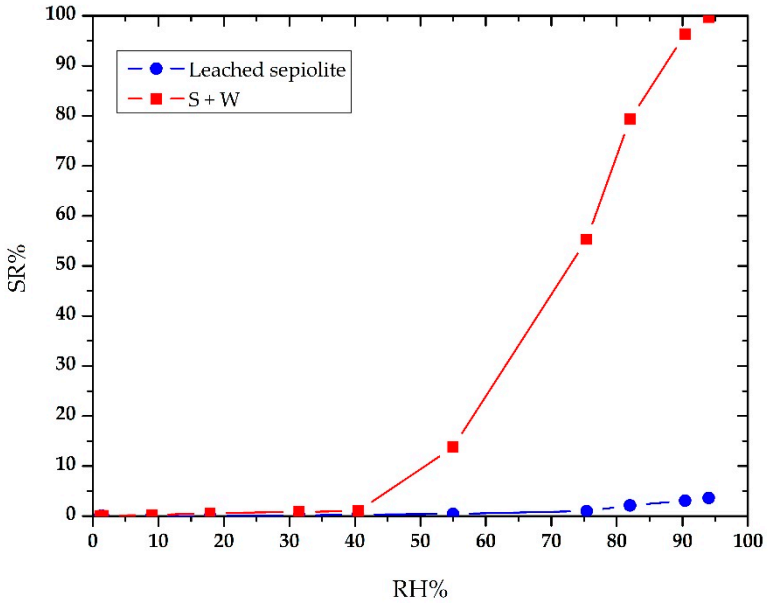

Figure 4. Sensors response to relative humidity (RH) at room temperature: leached sepiolite and tungsten-doped. Reprinted with permission from [20].

The abundance of the metal salts and inorganic clay are considered to be economically promising for the preparation of tungsten oxide nanoparticles and for further development of the obtained powder for new applications. Our findings confirm this process is valid for the synthesis of different oxide nanopowders, such as tungsten and zinc oxide, which can be used as the sensing film in chemical sensors [14,19,20]. Moreover, handling of nanopowders is much easier once they are precipitated onto sepiolite substrate, limiting their dispersion in air.

Author Contributions: A.S.A., M.H. and J.-M.T. conceived and designed the experiments; A.S.A., A.E., M.H. and M.A. performed the experiments; All the Authors analyzed the data; A.S.A., A.M. and J.-M.T. wrote the paper.

Funding: The research received no external funding.

Acknowledgments: The authors thank the company Hűls and Capelli (Milano, Italy) for providing sepiolite.

Conflicts of Interest: The authors declare that no conflict of interest exists.

References

1. Georg, A.; Graf, W.; Wittwer, V. Switchable windows with tungsten oxide. *Vacuum* **2008**, *82*, 730–735. [CrossRef]
2. Meng, D.; Yamazaki, T.; Shen, Y.; Liu, Z.; Kikuta, T. Preparation of WO_3 nanoparticles and application to NO_2 sensor. *Appl. Surf. Sci.* **2009**, *256*, 1050–1053. [CrossRef]
3. Tesfamichael, T.; Arita, M.; Bostrom, T.; Bell, J. Thin film deposition and characterization of pure and iron-doped electron-beam evaporated tungsten oxide for gas sensors. *Thin Solid Films* **2010**, *518*, 4791–4797. [CrossRef]
4. Ghasempour, R. Hybrid multiwalled carbon nanotubes and trioxide tungsten nanoparticles for hydrogen gas sensing. *J. Phys. D Appl. Phys.* **2009**, *42*, 165105. [CrossRef]
5. Pérez-Cadenas, A.; Moreno-Castilla, C.; Maldonado-Hódar, F.; Fierro, J. Tungsten oxide catalysts supported on activated carbons: Effect of tungsten precursor and pretreatment on dispersion, distribution, and surface acidity of catalysts. *J. Catal.* **2003**, *217*, 30–37. [CrossRef]
6. Azimirad, R.; Khosravi, P.; Moshfegh, A. Synthesis of $W_{17}O_{47}$ nanothick plates with preferred orientation and their photocatalytic activity. *Surf. Interface Anal.* **2011**, *43*, 1397–1402. [CrossRef]
7. Sun, X.; Liu, Z.; Cao, H. Electrochromic properties of N-doped tungsten oxide thin films prepared by reactive DC-pulsed sputtering. *Thin Solid Films* **2011**, *519*, 3032–3036. [CrossRef]
8. Schubert, W.; Lassner, E. Production and characterization of hydrogen-reduced submicron tungsten powders. Part I: State of the art in research, production and characterization of raw materials and tungsten powders. *Int. J. Refract. Met. Hard Mater.* **1991**, *10*, 133–141. [CrossRef]
9. Aegerter, M.A.; Avellaneda, C.O.; Pawlicka, A.; Atik, M. Electrochromism in materials prepared by the sol-gel process. *J. Sol-Gel Sci. Technol.* **1997**, *8*, 689–696. [CrossRef]
10. Santato, C.; Odziemkowski, M.; Ulmann, M.; Augustynski, J. Crystallographically oriented mesoporous WO_3 films: Synthesis, characterization, and applications. *J. Am. Chem. Soc.* **2001**, *123*, 10639–10649. [CrossRef] [PubMed]
11. Losier, P.; Ashrit, P. Flash evaporated tungsten oxide thin films for electrochromic applications. *J. Mater. Sci. Lett.* **2003**, *22*, 1095–1098. [CrossRef]
12. Palgrave, R.G.; Parkin, I.P. Chemical vapour deposition of titanium chalcogenides and pnictides and tungsten oxide thin films. *New J. Chem.* **2006**, *30*, 505–514. [CrossRef]
13. Regragui, M.; Addou, M.; Outzourhit, A.; Bernede, J.; El-Idrissi, E.; Benseddik, E.; Kachouane, A. Preparation and characterization of pyrolytic spray deposited electrochromic tungsten trioxide films. *Thin Solid Films* **2000**, *358*, 40–45. [CrossRef]
14. Esteban-Cubillo, A.; Tulliani, J.-M.; Pecharromán, C.; Moya, J.S. Iron-oxide nanoparticles supported on sepiolite as a novel humidity sensor. *J. Eur. Ceram. Soc.* **2007**, *27*, 1983–1989. [CrossRef]
15. Ding, Z.; Frost, R.L. Study of copper adsorption on montmorillonites using thermal analysis methods. *J. Colloid Interface Sci.* **2004**, *269*, 296–302. [CrossRef] [PubMed]
16. Hassan, M.; Afify, A.S.S.; Ataalla, M.; Mohammed, A.; Staneva, A.; Dimitriev, Y.; Tulliani, J.M.C. Preparation and characterization of a zinc oxide nanopowder supported onto inorganic clay. *J. Chem. Technol. Metall.* **2016**, *51*, 168–172.
17. Miura, A.; Nakazawa, K.; Takei, T.; Kumada, N.; Kinomura, N.; Ohki, R.; Koshiyama, H. Acid-, base-, and heat-induced degradation behavior of Chinese sepiolite. *Ceram. Int.* **2012**, *38*, 4677–4684. [CrossRef]
18. Valentín, J.; López-Manchado, M.; Rodríguez, A.; Posadas, P.; Ibarra, L. Novel anhydrous unfolded structure by heating of acid pre-treated sepiolite. *Appl. Clay Sci.* **2007**, *36*, 245–255. [CrossRef]
19. Hassan, M.; Afify, A.S.; Tulliani, J.M. Synthesis of ZnO nanoparticles onto sepiolite needles and determination of their sensitivity toward humidity, NO_2 and H_2. *J. Mater. Sci. Technol.* **2016**, *32*, 573–582. [CrossRef]

20. Afify, A.S.; Hassan, M.; Piumetti, M.; Peter, I.; Bonelli, B.; Tulliani, J.-M. Elaboration and characterization of modified sepiolites and their humidity sensing features for environmental monitoring. *Appl. Clay Sci.* **2015**, *115*, 165–173. [CrossRef]
21. Yebra-Rodriguez, A.; Martin-Ramos, J.D.; Del Rey, F.; Viseras, C.; Lopez-Galindo, A. Effect of acid treatment on the structure of sepiolite. *Clay Miner.* **2003**, *38*, 353–360. [CrossRef]
22. Fuhr, J.R.; Wiese, W.L.; Lide, D.R. *CRC Handbook of Chemistry and Physics*, 90th ed.; Lide, D.R., Haynes, W.M., Eds.; CRC Press Publisher: Boca Raton, FL, USA, 2009; p. 1978. ISBN 978-1-4200-9084-0.